Was the extended rainy winter 2018/2019 over the Middle and Lower reaches of the Yangtze River driven by anthropogenic forcing

Was the Extended Rainy Winter 2018/19 over the Middle and Lower Reaches of the Yangtze River Driven by Anthropogenic Forcing?

Zhiyuan Hu, Haiyan Li, Jiawei Liu, Shaobo Qiao, Dongqian Wang, Nicolas Freychet, Simon F. B. Tett, Buwen Dong, Fraser C. Lott, Qingxiang Li, and Wenjie Dong

AFFILIATIONS: Hu, H. Li, Qiao, Q. Li, and W. Dong—School of Atmospheric Sciences, and Key Laboratory of Tropical Atmosphere–Ocean System, Ministry of Education, Sun Yat-sen University, and Southern Marine Science and Engineering Guangdong Laboratory, Zhuhai, China; **Liu**—Collaborative Innovation Center on Forecast and Evaluation of Meteorological Disasters (CIC-FEMD)/Key Laboratory of Meteorological Disasters, Ministry of Education (KLME)/Joint International Research Laboratory of Climate and Environment Change (ILCEC), Nanjing University of Information Science and Technology, Nanjing, China; **Wang**—National Climate Center, China Meteorological Administration, Beijing, China; **Freychet and Tett**—School of Geosciences, University of Edinburgh, Edinburgh, United Kingdom; **B. Dong**—National Centre for Atmospheric Science, Department of Meteorology, University of Reading, United Kingdom; **Lott**—Met Office Hadley Centre, Exeter, United Kingdom

CORRESPONDING AUTHOR: Dr. Shaobo Qiao, qiaoshb3@mail.sysu.edu.cn

DOI:10.1175/BAMS-D-20-0127.1

A supplement to this article is available online (10.1175/BAMS-D-20-0127.2)

Anthropogenic forcing reduced the probability of rainfall amount in the extended rainy winter of 2018/19 over the middle and lower reaches of the Yangtze River, China, by ~19%, but exerted no influence on the excessive rainy days, based on HadGEM3-GA6-N216 ensembles. Instead the natural variability played a large and important role in this event.

During December 2018 to February 2019, the middle and lower reaches of the Yangtze River Valley (MLYRV) experienced an unprecedentedly extended rainy extreme weather event. This extreme event had more than 50 rainy days over the MLYRV in 2018/19 winter, resulting in a dramatic decrease in sunshine hours. According to the records from the China Meteorological Administration (CMA), daily-mean sunshine duration was less than 2 h during this event in many stations, reaching the lowest record in historical observations since 1961. This has led to severe impacts on natural systems, such as reduced agriculture productivity and increased load on power system supplies and transportations, and on human health (Liu et al. 2020). As such, this extended rainy event was defined as one of the top 10 extreme weather and climate events over China in 2019 by the CMA (http://www.cma.gov.cn/2011xwzx/2011xqxxw/2011xqxyw/202001/t20200103_543940.html).

Before this extreme event occurred (about September 2018), the tropical Pacific entered into a weak El Niño state (see Fig. ES1a in the online supplemental material), which favors a westward shift of the western Pacific subtropical high (WPSH) and excessive rainfall over the MLYRV (Wang et al. 2000; Wu et al. 2003; Zhou and Wu 2010). Anthropogenic warming since preindustrial times has been found to have affected extreme rainfall over East Asia, intensifying particularly short-term extreme rainfall (Burke et al. 2017; Zhang et al. 2007, 2017; Min et al. 2011; Westra et al. 2014; Dong et al. 2020). The aim of this study is to investigate whether anthropogenic warming changed the likelihood of the extended rainy winter of 2018/19.

Data and methods.

Daily rainfall observations for the period of 1961–2019 from ~2,400 stations are obtained from the CMA, and interpolated into 0.5° × 0.5° grid cells with the thin plate spline method (Shen et al. 2010). To analyze circulation fields associated with this event, monthly wind and geopotential height datasets from the NCEP–NCAR reanalysis (Kalnay et al. 1996) are used.

Simulations at 0.56° × 0.83° horizontal resolution with 85 vertical levels from the Met Office HadGEM3-GA6-N216 model (Ciavarella et al. 2018) are employed to assess anthropogenic influences on the probability of this extreme event. These simulations are driven by observed monthly sea surface temperature (SST) and sea ice concentration (SIC) from the Hadley Centre Sea Ice and Sea Surface Temperature dataset (Rayner et al. 2003) with both natural and anthropogenic forcings (HistoricalExt), and with natural forcing only for which anthropogenic contributions to the observed SST and SIC are removed (HistoricalNatExt). More details about the forcings used can be found in Christidis et al. (2013). Each experiment comprises an ensemble of 15 initial-condition simulation members for the period of 1960–2013 from which 525 members are extended up to 2019. This study particularly uses the 2018/19 winter simulations. Extreme rainfall events at local to regional spatial scales can be influenced greatly by internal climate variability, and the large ensemble of initial-condition simulations helps obtain reliable attribution results by providing a more adequate sampling of internal variability (Li et al. 2019).

The 2018/19 winter rainfall event is concentrated in 27°–32°N, 112°–122°E (Fig. 1a) and so this region is the focus of the analysis. Both the number of days with rainfall as well as the cumulative rainfall amount are considered. A rainy day is a day with more than 1 mm of precipitation, including rain and snow. The total number of rainy days and accumulated rainfall amount are computed for each winter (December to February) during 1961/62–2018/19, and are expressed as anomalies relative to the 1961/62–2010/11 climatology for both observations and simulations.

To test the reliability of model simulations, a Kolmogorov–Smirnoff (K–S) test comparing the distributions of observed and simulated anomalies of the number of rainy

Fig. 1. (facing page) (a),(b) Observed rainy days anomaly and rainfall amount anomaly in 2018/19 winter relative to the 1961/62–2010/11 climatology. (c),(d) Observed regional-mean rainy day anomaly and rainfall amount anomaly over the MLYRV in each winter for 1961/62–2018/19. (e),(f) Return periods and associated 95% confidence intervals for anomalies of regional-mean rainy days and rainfall amount, where the red dot denotes the value in 2018/19 winter. (g) 2018/19 winter 850-hPa moisture flux anomaly (arrows; g m^{-1} s^{-1} Pa^{-1}) and convergence (shaded; 10^{-7} g m^{-2} s^{-1} Pa^{-1}) 5,860 gpm contours of 500-hPa height for 2018/19 winter (red line) and climatology (blue line). (h) 500-hPa height anomalies in 2018/19 winter (contours; gpm). The regression of 500-hPa height anomalies onto the standardized rainy day number anomaly for 1961/62–2010/11 is also shown (shaded; gpm), where the dotted area is the region exceeding the 95% confidence level.

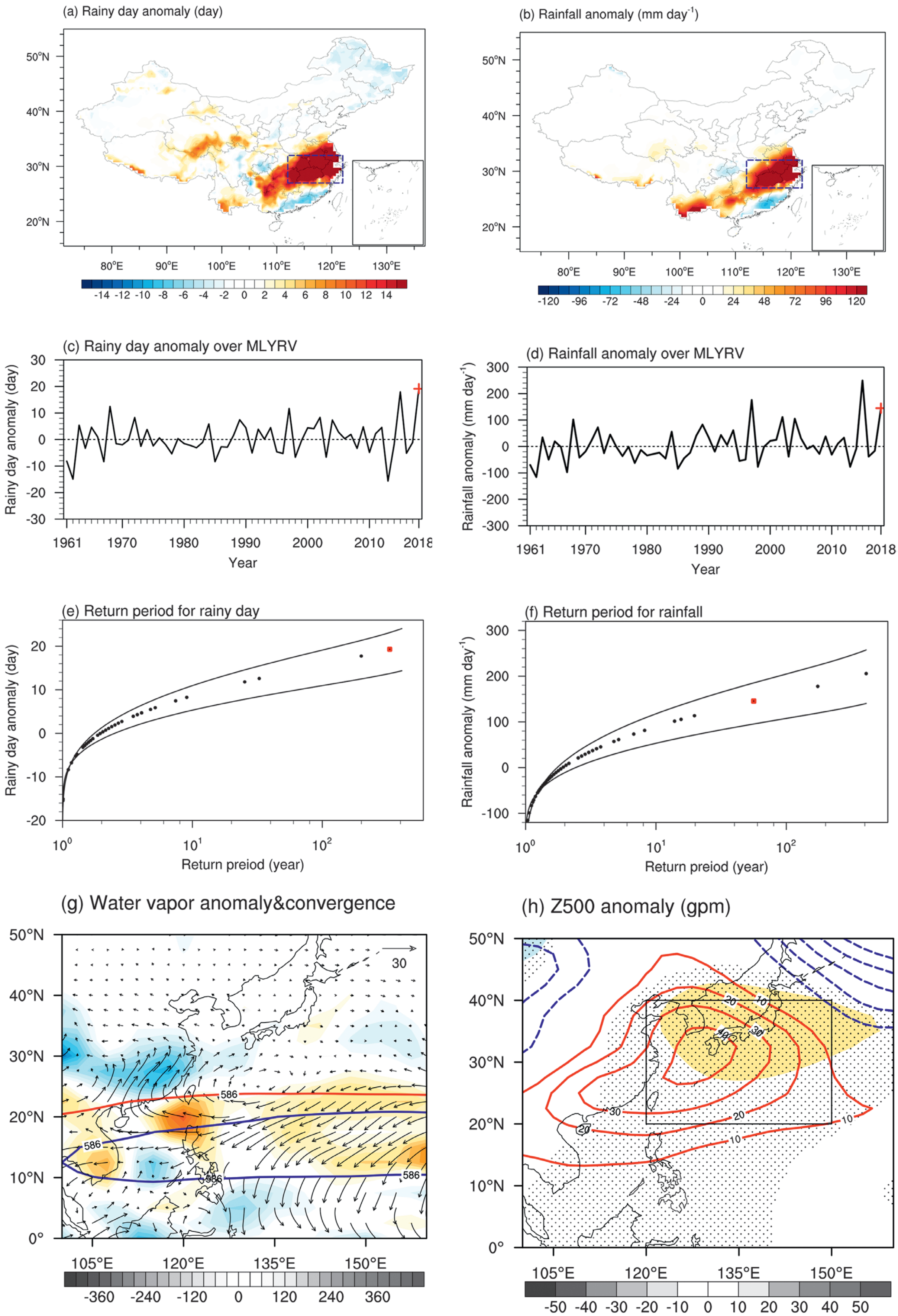
(a) Rainy day anomaly (day)
(b) Rainfall anomaly (mm day-1)
50°N
40°N
30°N
20°N
80°E
90°E
100°E
110°E
120°E
130°E
-14 -12 -10 -8 -6 -4 -2 0 2 4 6 8 10 12 14
-120 -96 -72 -48 -24 0 24 48 72 96 120
(c) Rainy day anomaly over MLYRV
Rainy day anomaly (day)
1961 1970 1980 1990 2000 2010 2018
Year
(d) Rainfall anomaly over MLYRV
Rainfall anomaly (mm day-1)
(e) Return period for rainy day
(f) Return period for rainfall
Return preiod (year)
(g) Water vapor anomaly&convergence
586
30
105°E
120°E
135°E
150°E
-360 -240 -120 0 120 240 360
(h) Z500 anomaly (gpm)
10
20
30
40
-50 -40 -30 -20 -10 0 10 20 30 40 50

days and rainfall amount is used. As both the number of rainy day and rainfall amount anomaly follow closely a normal distribution according to the F test for variances and K–S test (Figs. ES1d,e), Gaussian fits are used to quantify the occurrence probabilities and return periods of the number of rainy days and rainfall amount for 2018/19 in both observations and simulations with and without anthropogenic influence. Then, the risk ratio comparing the occurrence probability of the extended rainy event is computed, and the corresponding 5%–95% confidence interval are estimated via a bootstrapping procedure for 1,000 times, in which 525 samples are drawn from the 525 ensemble members with each time replacement.

Results.

The observations show significant positive anomalies in rainy days (Fig. 1a) and rainfall amount (Fig. 1b) over the MLYRV during 2018/19 winter. The regional-mean rainy days anomaly is more than 19 days relative to the 1961/62–2010/11 climatology, approaching 1.5 times the long-term mean value and breaking the historical record since 1961/62 (Fig. 1c). The regional-mean rainfall amount anomaly observed over the MLYRV exceeds 140 mm (Fig. 1b), which is the third wettest event during the whole period (Fig. 1d). In terms of return periods, rainy days and rainfall amount anomalies are greater than 100 (Fig. 1e) and 20 years (Fig. 1f) respectively, indicating the unusual rareness of an extended rainy event like the 2018/19 winter.

Although this extreme rainfall event occurred during a weak El Niño event, it is primarily driven by a persistent northwestward shift of the WPSH, as evidenced by the geopotential height contours of 5,860 gpm at 500 hPa extending to southern China (~22°N), about 5°–8°N of its climatological mean position (Fig. 1g). The associated low-level southwesterly winds over the northwest side of WPSH carry warm moist air that converges over the MLYRV, producing more-than-normal rainy days and rainfall amount in this region. Correspondingly, the positive 500-hPa height anomalies over the northwestern Pacific are obvious in 2018/19 winter, as supported by the regional-mean (20°–40°N, 120°–150°E) height anomaly that is as high as +24 gpm (Fig. 1h). The magnitude of the 500-hPa height anomalies over the northwestern Pacific in 2018/19 winter is about 2 times larger than that in regression pattern for 1961/62–2010/11, consistent with the record-breaking rainy day anomaly in this winter (Fig. 1a).

The HadGEM3-A-N216 model simulations for 1961/62–2012/13 reasonably capture the observed rainy day and rainfall amount variabilities (Figs. 2a,b). The distributions of rainy day and rainfall amount anomalies are comparable in model simulations and observations. Further, the observations fall within the range of model simulations. A K-S test reveals that the distributions of simulated and observed anomalies during 1961/62–2012/13 are statistically indistinguishable at 95% confidence level (p value = 0.39 for rainy day; p value = 0.31 for rainfall amount). Overall, the model provides reasonably well simulations of rainy day and rainfall amount over the MLYR that enable a reliable attribution analysis.

Although distributions of rainy day anomalies exhibit a small drying shift from HistoricalNatExt to HistoricalExt, they are very close in the upper tails where the number of rainy days in 2018/19 winter is observed. In particular, 7 of 525 ensemble members exceeds the observed anomaly of 19 days in both HistoricalNatExt and HistoricalExt. Correspondingly, the occurrence probability is 0.12 for both HistoricalNatExt (0.001–0.025) and HistoricalExt (0.002–0.024), with a risk ratio of 1.00 (0.90–1.18). The associated return period is estimated to be about 86 years (56–131 years; 5th–95th percentiles) in both ensembles, indicating that the anthropogenic forcing has relatively little influence on the rainy day anomaly (Fig. 2e), which might be a manifestation of the large local-to-regional internal variability.

Although the observed rainfall anomaly of 145 mm is slightly more likely without anthropogenic warming, the changed distribution between HistoricalNatExt and HistoricalExt is similar to that for rainy day anomalies (Fig. 2d). Correspondingly, the an-

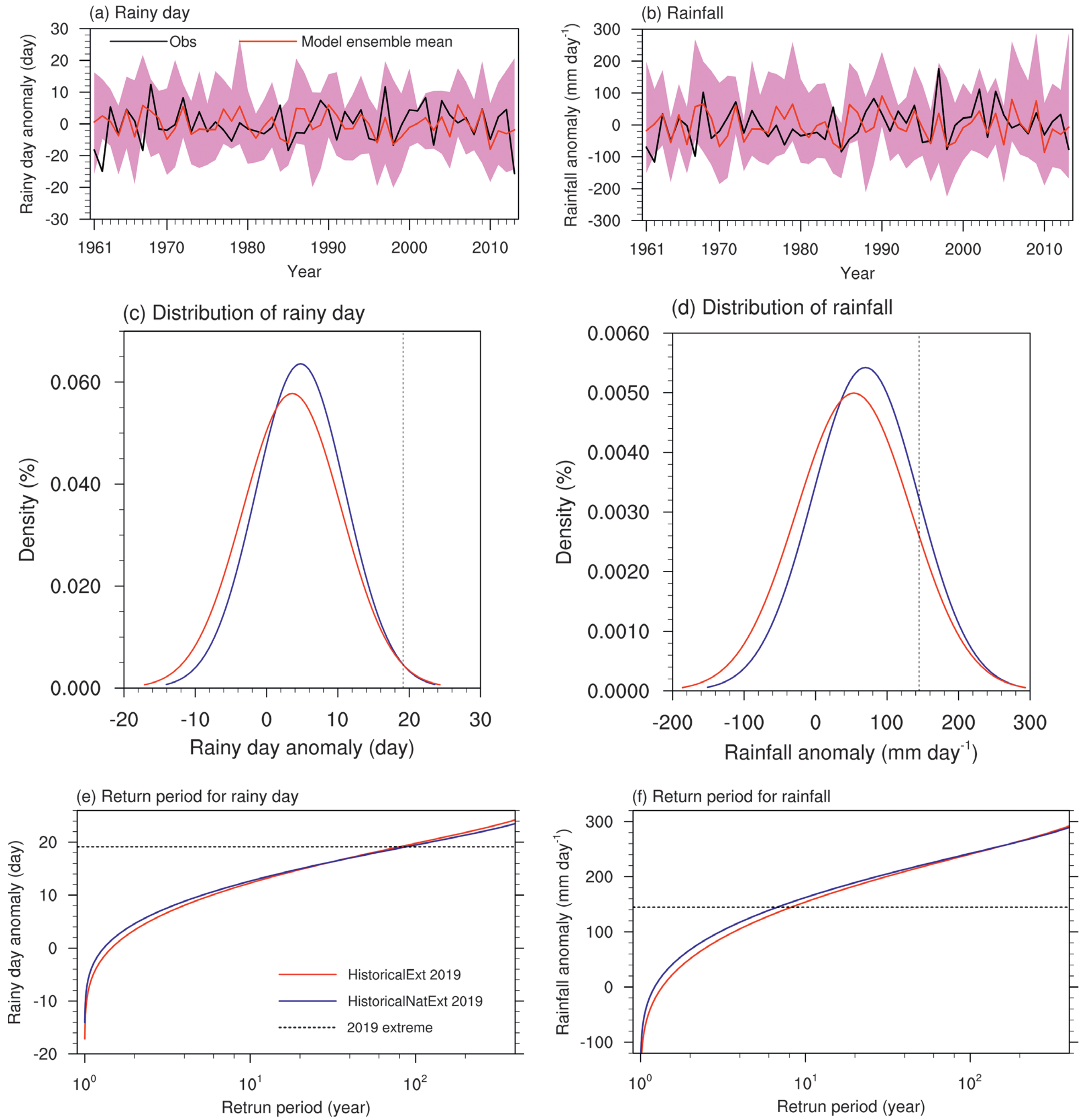

Fig. 2. (a),(b) Time series of observed (blue line) and simulated ensemble mean (red line) of rainy day anomaly and rainfall amount anomaly over the MLYRV in each winter for 1961/62–2012/13, with 15-member spread shown as light pink shading. (c),(d) Probability density function, using Gaussian fits, of rainy days anomaly and rainfall amount anomaly in 2018/19 winter with 525-member HistoricalExt (red line) and HistoricalNatExt (blue line) simulations. The dashed line denotes the observed 2018/19 winter. (e),(f) As in (c),(d), but for return periods.

thropogenic forcing is estimated to have decreased the occurrence probability from 0.16 (0.09–0.19) in HistoricalNatExt to 0.13 (0.07–0.18) in HistoricalExt, with a risk ratio of 0.81 (0.75–0.99). Compared to observations, the return period (~10 years) in rainfall amount anomalies is significantly decreased in model simulations (Fig. 1f vs Fig. 2f). The obviously different return period for rainfall amount anomaly between the simulations and observations is associated with the overestimated rainfall interannual variability in simulations (Figs. ES1d,e). Moreover, the circulation pattern anomalies are consistent regardless of the presence of anthropogenic warming (Figs. ES1b,c). These different lines of evidence suggest that the natural variability played a large and important role in the extended rainy event in 2018/19 winter over MLYRV.

Conclusions and discussion.

In 2018/19 winter, an unprecedented extended rainy event occurred over the middle and lower reaches of the Yangtze River Valley, with more than 50 rainy days breaking the historical record since 1961/62. This event was primarily driven by persistent northwestward shift of the WPSH, where the associated low-level southwesterly winds could carry warm moist air that converges over the region. By analyzing two large ensemble simulations with and without the influence of anthropogenic warming from the HadGEM3-A-N216 model, we found that anthropogenic forcing has reduced the probability of rainfall amount in this event by ~19%, but exerted no influence on the excessive rainy days. Instead the natural variability played a large and important role in this event.

Generally, the extratropical land precipitation at monthly to seasonal time scales is dominated by atmospheric internal processes with external forcings (SST, SIC, etc.) played a secondary role (Hu et al. 2020). The shift of the PDF in 2018/19 winter, relative to the mean climatology, to wetter conditions for both rainy day and rainfall amount anomalies in both ensembles (Fig. 2c vs Fig. ES1e; Fig. 2d vs Fig. ES1d) suggests that this event is driven by the external forcings. This conclusion is consistent with the study of Liu et al. (2020), which further indicates that tropical Atlantic warming, interdecadal variation, and central tropical Pacific warming are three major factors leading to this extended rainy winter. Also, a drying shift of the probability density functions for anomalies of rainfall amount in HistoricalExt compared HistoricalNatExt suggests the anthropogenic signal is detected to some extent, and thus more work is necessary to separate the human influences on this shift (Power et al. 2013; Balan Sarojini et al. 2016).

Additionally, our conclusions are only based on daily observed rainfall from CMA and ensembles from a single atmospheric model forced by observed SST or SIC with and without anthropogenic warming. Multiple observational datasets (Hegerl et al. 2015) and a comparison with estimates from fully coupled models (Sun et al. 2014; Massey et al. 2015; Ren et al. 2020) are needed to test our results, as ocean–atmosphere interaction is important for East Asian climate (Wang et al. 2005).

Acknowledgments. This study was largely carried out during a workshop on Operational Attribution at Sun Yat-Sen University, China, sponsored by the U.K.–China Research and Innovation Partnership Fund through the Met Office Climate Science for Service Partnership China as part of the Newton Fund, the National Key R&D Program of China (Grant 2018YFC1507700) and the Natural Science Foundation of China (Grant 41975105). Z. H. was funded by the Natural Science Foundation of China (Grants 41905013 and 41805116), S. Q. was funded by the Natural Science Foundation of China (Grants 41905057 and 41875096) and the Postdoctoral Science Foundation of China (Grant 2018M640848), H. L. was funded by the Postdoctoral Science Foundation of China (Grant 2019M663204), J. L. is supported by the National Natural Science Foundation of China (Grants 41575077 and 41490643). N. F., S. F. B. T., B. D., and F. L. are all supported by the Met Office Climate Science for Service Partnership China as part of the Newton Fund.

References

Belan Sarojini, B., P. A. Stott, and E. Balck, 2016: Detection and attribution of human influence on regional precipitation. *Nat. Climate Change*, **6**, 669–675, https://doi.org/10.1038/nclimate2976.

Burke, C., and P. Stott, 2017: Impact of anthropogenic climate change on the East Asian summer monsoon. *J. Climate*, **30**, 5205–5220, https://doi.org/10.1175/JCLI-D-16-0892.1.

Christidis, N., P. A. Stott, A. A. Scaife, A. Arribas, G. S. Jones, D. Copsey, J. R. Knight, and W. J. Tennant, 2013: A new HadGEM3-A-based system for attribution of weather- and climate-related extreme events. *J. Climate*, **26**, 2756–2783, https://doi.org/10.1175/JCLI-D-12-00169.1.

Ciavarella, A., and Coauthors, 2018: Upgrade of the HadGEM3-A based attribution system to high resolution and a new validation framework for probabilistic event attribution. *Wea. Climate Extremes*, **20**, 9–32, https://doi.org/10.1016/j.wace.2018.03.003.

Dong, S., Y. Sun, and C. Li, 2020: Detection of human influence on precipitation extremes in Asia. *J. Climate*, **33**, 5293–5304, https://doi.org/10.1175/JCLI-D-19-0371.1.

Hegerl, G. C., and Coauthors, 2015: Challenges in quantifying changes in the global water cycle. *Bull. Amer. Meteor. Soc.*, **96**, 1097–1115, https://doi.org/10.1175/BAMS-D-13-00212.1.

Hu, Z.-Z., A. Kumar, B. Jha, and B. Huang, 2020: How much of monthly mean precipitation variability over global land is associated with SST anomalies? *Climate Dyn.*, **54**, 701–712, https://doi.org/10.1007/s00382-019-05023-5.

Kalnay, E., and Coauthors, 1996: The NCEP/NCAR 40-Year Reanalysis Project. *Bull. Amer. Meteor. Soc.*, **77**, 437–471, https://doi.org/10.1175/1520-0477(1996)077<0437:TNYRP>2.0.CO;2.

Li, C., F. Zwiers, X. Zhang, and G. Li, 2019: How much information is required to well constrain local estimates of future precipitation extremes? *Earth's Future*, **7**, 11–24, https://doi.org/10.1029/2018EF001001.

Liu, Y., Z. Hu, and R. Wu, 2020: Was the extremely wet winter of 2018/2019 in the lower reach of the Yangtze River driven by El Niño–Southern Oscillation? *Int. J. Climatol.*, https://doi.org/10.1002/joc.6591, in press.

Massey, N., and Coauthors, 2015: weather@home—Development and validation of a very large ensemble modelling system for probabilistic event attribution. *Quart. J. Roy. Meteor. Soc.*, **141**, 1528–1545, https://doi.org/10.1002/qj.2455.

Min, S., X. Zhang, F. Zwiers, and G. Hegerl, 2011: Human contribution to more-intense precipitation extremes. *Nature*, **470**, 378–381, https://doi.org/10.1038/nature09763.

Power, S., F. Delage, C. Chung, G. Kociuba, and K. Keay, 2013: Robust twenty-first-century projections of El Niño and related precipitation variability. *Nature*, **502**, 541–545, https://doi.org/10.1038/nature12580.

Rayner, N. A., D. E. Parker, E. B. Horton, C. K. Folland, L. V. Alexander, D. P. Rowell, E. C. Kent, and A. Kaplan, 2003: Global analyses of sea surface temperature, sea ice, and night marine air temperature since the late nineteenth century. *J. Geophys. Res.*, **108**, 4407, https://doi.org/10.1029/2002JD002670.

Ren, L., and Coauthors, 2020: Anthropogenic influences on the persistent night-time heat wave in summer 2018 over northeast China. *Bull. Amer. Meteor. Soc.*, **101**, S83–S88, https://doi.org/10.1175/BAMS-D-19-0152.1.

Shen, Y., A. Xiong, Y. Wang, and P. Xie, 2010: Performance of high-resolution satellite precipitation products over China. *J. Geophys. Res.*, **115**, D02114, https://doi.org/10.1029/2009JD012097.

Sun, Y., X. Zhang, F. W. Zwiers, L. C. Song, H. Wan, T. Hu, H. Yin, and G. Y. Ren, 2014: Rapid increase in the risk of extreme summer heat in eastern China. *Nat. Climate Change*, **4**, 1082–1085, https://doi.org/10.1038/nclimate2410.

Wang, B., R. Wu, and X. Fu, 2000: Pacific–East Asian teleconnection: How does ENSO affect East Asian climate? *J. Climate*, **13**, 1517–1536, https://doi.org/10.1175/1520-0442(2000)013<1517:PEATHD>2.0.CO;2.

Wang, B., Q. Ding, X. Fu, I.-S. Kang, K. Jin, J. Shukla, and F. Doblas-Reyes, 2005: Fundamental challenges in simulation and prediction of summer monsoon rainfall. *Geophys. Res. Lett.*, **32**, L15711, https://doi.org/10.1029/2005GL022734.

Westra, S., and Coauthors, 2014: Future changes to the intensity and frequency of short-duration extreme rainfall. *Rev. Geophys.*, **52**, 522–555, https://doi.org/10.1002/2014RG000464.

Wu, R., Z. Hu, and B. Kirtman, 2003: Evolution of ENSO-related rainfall anomalies in East Asia. *J. Climate*, **16**, 3742–3758, https://doi.org/10.1175/1520-0442(2003)016<3742:EOERAI>2.0.CO;2.

Zhang, X., F. Zwiers, G. Hegerl, F. Lambert, N. Gillett, S. Solomon, P. Stott, and T. Zozawa, 2007: Detection of human influence on twentieth-century precipitation trends. *Nature*, **448**, 461–465, https://doi.org/10.1038/nature06025.

Zhang, X., F. Zwiers, G. Li, H. Wan, and A. Cannon, 2017: Complexity in estimating past and future extreme short-duration rainfall. *Nat. Geosci.*, **10**, 255–259, https://doi.org/10.1038/ngeo2911.

Zhou, L., and R. Wu, 2010: Respective impacts of the East Asian winter monsoon and ENSO on winter rainfall in China. *J. Geophys. Res.*, **115**, D02107, https://doi.org/10.1029/2009JD012502.